SUPPORTING INFORMATION

to

Nucleotide and Nucleotide Sugar Analysis by LC-ESI-MS on Surface-Conditioned Porous Graphitic Carbon

Martin Pabst[a], Josephine Grass[a], Richard Fischl[a], Renaud Léonard[a], Chunsheng Jin[a], Georg Hinterkörner[b$], Nicole Borth[b], Friedrich Altmann[a*]

[a] Department of Chemistry and [b] Department of Biotechnology, University of Natural Resources and Applied Life Sciences (BOKU), Vienna, Austria;

Corresponding author, E-mail address: friedrich.altmann@boku.ac.at

Supporting Materials and Methods:

Materials

The common nucleotides and deoxynucleotides, NAD^+, $NADP^+$, NADH, NADPH, UDP-Glc, UDP-glucuronic acid (GlcUA), ADP-ribose, ADP-glucose, 3´-phosphoadenosine-5´-phosphosulfates (PAPS) and 2´-phosphoadenosine-5´-phosphosulfates (2´-PAPS), and ^{13}C-ATP were from Sigma Aldrich. UDP-Gal, CMP-Neu5Ac, GDP-Man, GDP-Fuc were from Kyowa-Hakko (Duesseldorf, Germany). UDP-xylose (precisely UDP-β-D-xylopyranose) and UDP-β-L-arabinopyranose were purchased from CarboService (Athens, GA, USA).

Cells and plants

CHO dhfr$^-$ cells (ATCC CRL-9096) were cultivated in spinner flasks in a 1:1 mixture of DMEM and Ham's F12 medium, supplemented with 4 mM L-glutamine, 0.25% soy peptone, 0.1% Pluronic F60, a protein-free additive (Polymun Scientific, Vienna) and hypoxanthine/thymidine stock solution, at 37°C, 7% CO_2 and 50 rpm.

Leaves of glass house-grown *Nicotiana benthamiana* were kindly provided by Pia Gattinger and Richard Strasser from the Department of Applied Genetics and Cell Biology. *Arabidopsis thaliana* leaves were taken from plants grown in soil for three weeks as described [1]. The

GDP-mannose epimirase (GME) RNAi construct was obtained successively using the vectors pSAT4.35SP.RNAi and pRCS-ocs-nptII [2]. The full open reading frame of AT5G28840 was amplied with the primers GAAGATCTTCATGGGAACTACCAATGGAAC and GGAATTCCTCACTCTTTT CCATCAGCC or CGGGATCCCGATGGGAACTACCAATGGAAC and GGGGTACCCC TCACTCTTTTCCATCAGCC. GME RNAi *Arabidopsis* plants were obtained by floral dipping and selected for kanamycine resistance [1].

Alternative extraction procedures

In an alternative quenching procedure, cells were transferred to a fivefold volume of 60 % (v/v) methanol containing 0.85% ammonium bicarbonate at -80°C as recommended [3]. The centrifugation step was changed to 1 min at 1000 × g at 4°C, to minimize exposure of the cells to organic solvents.

Two alternative extraction procedures were tried with CHO cells. Extraction with perchloric acid was performed as described previously [4]. Also, we performed the elaborate method applied in a work on UDP-sugars from spinach cells [5], where lysis with NaF was followed by partition using chloroform : methanol : H_2O = 10 : 10 : 3 (weight of cells taken as H_2O). The suspension was stirred for 30 min at 4°C, centrifuged and the aqueous layer was immediately taken to analysis.

Extraction of analytes from plant samples

Plant tissue (5 – 50 mg) was homogenized with a ball mill grinder under liquid nitrogen and then suspended in 0.5 mL of 40 mM sodium fluoride. After about 10 sec incubation time, insoluble material was removed by centrifugation at 4°C 10,000 × g for 3 min. The nucleotides of the supernatant were purified by SPE on carbon cartridges as described above.

Bacterial cells (10^9 *E. coli* B21 cells grown in Luria-Bertani medium) received the same treatment as CHO cells, which sufficed to permit detection of CMP-KDO.

Peak quantitation using MassMap®

Prior to the identification of the molecules analyzed, low-intensity noise was removed to increase the speed of processing. The parameters employed for this step were chosen such that no significant signals were removed from the data sets. The noise-corrected data sets were subjected to so-called pepmap-analyses. In a first step, the data were automatically tested for

the presence of the molecules of interest. Given the nature of the analytes, the testing was restricted to singly charged ions.

Identification of each peak can be evaluated by the user, but this labor-intense step was often skipped for less important samples. For the identified and accepted molecules, the software automatically generated the following numbers: location of the chromatographic peak, deviation of the molecular mass from the given value and – last but not least - integral of the monoisotopic peak of the singly charged ions. In addition, the mean relative mass deviation of a selection of molecules was calculated in order to allow mass re-calibration and application of a narrow mass window during subsequent automated peak detection.

To verify the MassMap settings for peak identification and quantitation of analytes, the data sets were also processed "manually" with MassLynx by measuring the intensity of the base peak of the sum spectrum covering the entire analyte peak in the extracted ion chromatogram.

Column conditioning was performed with either 100 mM sodium sulfite or 100 mM H_2O_2 at a flow rate of 10 µL/min. New PGC columns were treated with sulfite for 6 h. Used PGC columns suffering of elevated backpressure or reduced retention were regenerated with 4 M trifluoroacetic acid (TFA) at 120`C for 3 h as described [6]. Columns were then rinsed with 0.1 M HCl for 30 min after which the column was placed for 30 min in an incubator at 100°C. Then the column was rinsed with distilled water and subjected to reductive conditioning for 2 h followed by two blank runs with formate buffer.

Other preparative and analytical procedures

As commercial ATP preparations – at least upon storage – contain some AMP and ADP, pure ATP was isolated by ion exchange chromatography on CarboPac 1 operated similar as described by Konishi et al. [7].

Prepurification of larger amounts of nucleotide sugars was performed by using a Hypercarb PGC column (3 × 150 mm, ThermoScientific) with UV-detection at 254 nm. Fractions containing the relevant UDP- or GDP-sugars were collected and further separated by weak anion exchange chromatography on a TSK DEAE 5PW column (7.5 x 75 mm; TOSOH bioscience, Stuttgart). Sugar-nucleotides were eluted with a gradient from 15-100 % 1 M ammonium acetate of pH 9 in water developed within 30 min at a flow rate of 2 mL/min. In both steps, fractions were checked by off-line ESI-MS for identification of peaks and purity. After weak anion exchange chromatography, relevant fractions were freeze dried and hydrolyzed with 1 M TFA at 100 °C for 1 h. Monosaccharides were analyzed by HPLC as anthranilic acid (AA) derivatives [8]. In addition to the conventional fluorescent format, the

AA-labeled sugars were subjected to LC-MS and LC-MS/MS analysis using 0.1% formic acid as solvent A. AA-rhamnose and AA-fucose cannot be separated, but their MS/MS spectra are sufficiently distinct to ensure correct assignment of the peaks (data not shown).

Enzymes for conversion or synthesis of nucleotide sugars

Mung bean microsomes, prepared from fresh sprouts as described recently [9], were used as source of Golgi-resident UDP-xylose epimerase [10]. Fresh mung bean sprouts (100 g) were homogenized at 4°C in 70 mL Tris-HCl buffer pH 7.3 containing 0.5 mM DTT, 1 mM EDTA, 250 mM sucrose and 0.5 mM phenylmethanesulfonyl fluoride. The suspension was filtered through Miracloth (Merck) and centrifuged at 3,000 g and 4°C for 20 minutes. The supernatant was ultracentrifugated at 100,000 g and 4°C for 75 minutes. The microsomal pellet was resuspended in 1 mL 50 mM MES KOH buffer pH 7.0 containing 0.5% Triton X-100 and used as enzyme source. For the enzymatic reaction of UDP-xylose epimerase, 2 nmol UDP-Arap or UDP-Xyl*p* respectively were incubated with the microsomal extract in 25 mM MES, pH 7.0 containing 20 mM $MnCl_2$ and 0,1% triton X-100 at room temperature for 2 h. After a prepurification step with the Hypercarb cartridge as described above, the enzymatic conversion was measured by PGC-LC-ESI-MS, as described above, injecting an equivalent of originally 25 pmol of the respective nucleotide sugar.

Recombinant rice UDP-arabinose mutase 3 (OsUAM3, UniProt Q6Z4G3) fused with a N-terminal His6-tag was expressed in *E. coli* BL21 (DE3) [7]. Recombinant OsUAM3 was purified through Ni-NTA agarose column (Qiagen, Vienna, Austria) according to manufacturer's instruction. To measure the enzymatic formation of UDP-Ara*f*, 5 nmol UDP-Ara*p* was incubated with purified recombinant OsUAM3 in 20 mM MES, pH 7.0 containing 5 mM MnCl2 at room temperature for 1 h. To measure enzymatic activity, samples were prepurified by the Hypercarb cartridge and analysed by PGC-LC-ESI-MS.

Supporting Results

Identification of selected nucleotide sugars (potentially Supporting Information)

UDP-galacturonic acid: In addition to UDP-glucuronic acid (UDP-GlcUA), a second peak having the mass and the MSMS spectrum of a UDP-hexuronic acid, presumably UDP-galacturonic acid (UDP-GalUA), occurs in extracts of plant tissues (SI Table 1). To substantiate our assumption, a mung bean sprouts extract was fractionated by strong anion exchange and graphitic carbon chromatography with UV detection. Relevant PGC fractions were subjected to LC-MS analysis to identify the one containing the putative UDP-GalUA. Monosaccharide analysis of this fraction revealed it to contain a substantial amount of GalUA. Thus, the first UDP-hexuronic peak was assigned as UDP-GalUA, which is an important precursor for the synthesis of pectic polysaccharides.

UDP-rhamnose: Similarly, the peak with the mass and fragment spectrum of a UDP-deoxyhexose was isolated and subjected to monosaccharide analysis as anthranilic acid derivative. In fact, the peak contained rhamnose, and in accordance with the plant metabolite network database (www.plantcyc.org) it can be assumed to be UDP-L-rhamnose. The biosyntheses of UDP-L-rhamnose starts from UDP-D-glucose, which is converted to UDP-4-keto-6-deoxy-D-glucose by a dehydratase. In *A. thaliana* and tobacco leaves, a small peak with the mass of this intermediate was detected, which in MS/MS gave fragments for UMP and UDP and a neutral loss fitting to keto-deoxy-hexose. Thus, we tentatively assigned this peak as UDP-4-keto-6-deoxy-D-glucose.

UDP-L-arabinofuranose: The elution position of UDP-arabinofuranose (UDP-Ara*f*), which is assumed to be the true donor substrate for arabinosyltransferases [11], was obtained by incubating UDP-Ara*p* with recombinant rice UDP-Ara mutase (Fig. 4). The equilibrium of this reaction lies on the side of the pyranose form, so that the mixture contained only about 10 % of UDP-Ara*f*. Consequently, an only small peak for UDP-Ara*f* was found in plant leaves (SI Table 1, Fig. 4).

Attempts to detect UDP-Ara mutase activity in mung bean sprout microsomes failed but revealed the activity of UDP-xylose epimerase, as this enzyme likewise uses UDP-Ara*p* as substrate.

A close look at the elution profile of UDP-pentoses reveals one or even two additional, small peaks (SI Table 1, Fig. 4). One of these peaks may represent UDP-apiose, a compound involved in formation of rhamnogalacturonan II [12].

GDP-L-galactose: A peak briefly behind that of GDP-Man exhibited a very similar MS/MS spectrum. Indeed, HPLC monosaccharide analysis of the isolated peak revealed it to contain Gal (data not shown). While we did not determine the DL-configuration of this hexose, it appears reasonable to assign the peak as GDP-L-Gal. L-galactose is the product of GDP-D-mannose-3,5-epimerase, for which an intermediate product (just epimerization of the 5 position) is L-gulose [13]. The GDP-L-galactose peak actually had a shoulder (SI Figure 3), which we presume to represent the intermediary metabolite GDP-L-gulose as the area ratios resemble that reported for the *in vitro* synthesis of these two sugars [14] . The presence of gulose could not be confirmed by monosaccharide analysis as unfortunately the gulose derivative elutes close to the omnipresent glucose. In *A. thaliana* plants transfected with an RNAi construct against GDP-D-mannose-3,5-epimerase, the entire double peak of UDP-Gal/UDP-Gul amounted to only 10-20 % of that in wild type plants (SI Figure 3). In return, GDP-Man, the substrate for the missing epimerase, was apparently accumulating.

UDP-sulfoquinovinose: This nucleotide serves for the synthesis of the membrane lipid sulfoquinovosyldiacylglycerol in plants (www.plantcyc.org). A nucleotide sugar of the respective mass (and MSMS spectrum, not shown) was found in mung bean, *A. thaliana* and tabacco but not in CHO extracts (SI Table 1)

ADP-ribose and ADP-ribose phosphate: ADP-ribose may arise from NAD^+ breakdown or from degradation of poly(ADP-ribosyl)ated proteins [15]. The MouseCyc database (http://mousecyc.jax.org) knows of a ADP ribose 1',2´-phosphate, which we could not find in any of our samples. However, considerable amounts of ADP-ribose phosphate, possibly a byproduct of RNA splicing [16] were detected in all eukaryotic samples. The second messenger cyclic ADP-ribose, just like NAADP, could not be found.

ADP-glucose, the sugar donor of starch and glycogen synthesis, was found in plant and animal samples. Although isobaric with GDP-fucose, ADP-glucose is easily distinguished by its retention time and, of course, MS/MS fragments.

Further ADP sugars were found in bacteria and, very unexpectedly, also in mammalian tissue (see below).

Bacterial nucleotide sugars: *E. coli* was used to verify whether the PGC-based procedure allowed to find the extremely labile CMP-KDO (SI Figure 2). Analysis of the bacterial extract revealed many other nucleotide sugars such as dTDP-rhamnose [17], a second dTDP-deoxyhexose (probably dTPD-fucose) (http://ecocyc.org), dTDP-4-deoxy-4-acetamido-fucose (isobaric with GDP-fucose), UDP-4-deoxy-4-formamido-L-arabinose (but not UDP-β-4-deoxy-4-amino-L-arabinose) [18] and ADP-heptose to name just the most prominent.
Surprisingly, an ADP-heptose with the same elution position and also an ADP-heptose phosphate (or sulfate) were found in mouse liver extract (data not shown), for which we could not find any explanation in the literature or the mouse metabolism databank (http://mousecyc.jax.org).

Supporting Tables:

Supporting Table 1: Occurrence of nucleotides in leaves of *Arabidopsis thaliana* or *Nicotiana benthamiana*, in CHO cells and *Escherichia coli* K12. "RRT" is the relative net retention time based on that of UDP-glucose. Note that peaks with an RRT larger than 2 are not eluting with the linear gradient. The evidence for peak assignment was either a commercial standard ("Std"), the MS/MS spectrum or literature data as specified in the Supporting results. In the latter cases, assignment is mostly rated as tentative ("tent").

For legend see previous page

Nucleotide	evidence	exact mass	RRT	*A. thal.*	*N. bent.*	CHO	*E. coli*
				pmol / g fresh tissue	pmol / g fresh tissue	pmol / 10^6 cells	relative to UDP-Glc
CMP	Std	323.052	0.70	0.7	0.9	0.1	0.6
iso-CMP	MS/MS	323.052	1.24	0.6	0.2		
CDP	Std	403.018	0.76	1.9	3.0	1.1	1.2
CTP	Std	482.985	0.76	2.3	0.5	1.7	1.4
UMP	Std	324.036	0.72	7.7	3.0	0.3	0.7
iso UMP	MS/MS	324.036	1.24	1.4	1.4		
iso UMP	MS/MS	324.036	1.40	2.0			
UDP	Std	404.002	0.77	12.9	7.9	3.3	3.8
UTP	Std	483.969	0.80	11.6	4.7	3.8	2.7
dCMP	Std	307.057	0.83			0.3	
dCDP	Std	387.023	0.64			0.1	
dCTP	Std	466.990	0.81			0.4	
dTMP	Std	322.057	1.20				
dTDP	Std	402.023	1.18			0.3	10.9
dTTP	Std	481.989	1.16		1.0	0.3	4.1
GMP	Std	363.058	1.35	4.1	11.3	0.7	16.1
iso GMP	MS/MS	363.058	1.92	3.8	10.9	tr	tr
iso GMP	MS/MS	363.058	2.19	4.2	1.0		
GDP	Std	443.024	1.40	7.3	16.1	6.7	23.5
GTP	Std	522.991	1.41	1.7	5.0	9.8	4.2
dGMP	Std	347.063	1.78				
dGDP	Std	427.030	1.81	tr		tr	
dGTP	Std	506.996	1.78	tr			
AMP	Std	347.063	1.44	24.7	57.5	2.4	27.4
iso AMP	MS/MS	347.063	2.10	1.2	11.0		0.8
iso AMP	MS/MS	347.063	3.01	2.6	11.9		5.2
ADP	Std	427.030	1.51	57.7	112	25.0	140
3´,5´-ADP	Std, MS/MS	427.030	0.81	1.9	0.9		tr
2´,5´-ADP	Std, MS/MS	427.030	1.01	1.1			
ATP	Std	506.996	1.51	47.4	63.6	43.1	63.3
dAMP	Std	331.068	1.80				6.0
dADP	Std	411.035	1.87			0.4	34.6
dATP	Std	491.001	1.83			0.6	12.2
PAPS	Std	506.986	1.16	3.4	tr	0.1	
2´-PAPS	Std	506.986	1.16				
APS	tent	427.020	1.85				
2,3-cAMP	MS/MS	329.051	2.60		0.9		
3,5-cAMP	Std	329.051	2.65		tr		
NAD+	Std	663.109	2.63	36	163	3.0	299
NADH	Std	665.125	2.35			[1)]	
NADP+	Std	743.076	2.55	178	578	3.3	167
NADPH	Std	745.091	2.27			0.5	
NAAD	Std	664.093	2.28	90	4.0	tr	3.1

[1)] Both NADH and NADPH could be found in extracts of mouse liver

Supporting Table 2: Occurrence of nucleotide sugars in leaves of *Arabidopsis thaliana* or *Nicotiana benthamiana*, in CHO cells and *Escherichia coli* K12. See Supporting Table 1 for explanations. Abbrevations for nucleotide sugars are: UDP-S-Quin, UDP-sulfoquinovose; UDP-kd-Glc, UDP-4-keto-6-deoxy-glucose; UDP-Ara4FN, UDP-4-deoxy-4-formamido-L-arabinose; ADP-gm-Hep, ADP-glycero-manno-heptose; dTDP-Fuc4Nac, dTPD-N-acetyl-fucosamine.

Nucleotide sugar	evidence	exact mass	RRT	*A. thal.*	*N. bent.*	CHO	*E. coli*
				pmol / g fresh tissue	pmol / g fresh tissue	pmol / 10^6 cells	relative to UDP-Glc
UDP-GalUA	MS/MS, HPLC	580.027	0.79	4.0	2.9		
UDP-GlcUA	Std	580.027	0.81	12.4	11.7	3.0	10.9
UDP-D-Gal	Std	566.047	0.94	96.1	45.1	1.6	
UDP-D-Glc	Std	566.047	1.00	**280**	**168**	**5.3**	**100**
UDP-Hex-3	MS/MS	566.047	0.85				
UDP-GalNAc	Std	607.076	1.01			[1]	
UDP-GlcNAc	Std	607.076	1.02	38.9	26.2	17.4	52.7
UDP-HexNAc-3	MS/MS	607.076	0.86				0.9
UDP-HexNAc-4	MS/MS	607.076	0.96				8.4
UDP-Rha	MS/MS, HPLC	550.054	0.90	19.4	11.4		1.1
UDP-S-Quin	MS/MS, Lit	630.016	0.98	3.4	7.4		
UDP-kd-Glc	MS/MS, Lit, tent	548.043	1.10	tr			
UDP-L-Ara*p*	Std	536.037	1.06	20.1	9.2	0.1	
UDP-L-Xyl	Std	536.037	1.00	15.7	9.6	0.2	
UDP-L-Ara*f*	Std	536.037	1.05	2.4	0.8		
UDP-Pen-4	MS/MS	536.037	1.10	0.8	tr		
UDP-Pen-5	MS/MS	536.037	0.90	tr			
UDP-Ara4FN	MS/MS, Lit, tent	563.055	0.96				11.0
GDP-D-Man	Std	605.067	1.54	13.6	30.6	1.5	
GDP-L-Gal	MS/MS, HPLC	605.067	1.64	3.1	7.1		
GDP-L-Gul	MS/MS, Lit, tent	605.067	1.67	1.0	2.4		
GDP-Glc	MS/MS, Lit, tent	605.067	1.71				0.5
GDP-L-Fuc	Std	589.074	1.73	6.6	9.5	1.8	1.0
ADP-D-Rib-P	MS/MS, tent	639.038	1.28	1.2	1.0	0.1	
ADP-D-Rib	Std	559.072	1.80	2.1	3.7	0.3	6.9
ADP-D-Glc	Std	589.074	1.83	1.7	3.4	0.1	
ADP-Hex-2	MS/MS	589.074	1.61	0.5	tr		
ADP-Hex-3	MS/MS	589.074	1.68			0.2	
ADP-gm-Hep	MS/MS, Lit	619.093	1.67				15.1
CMP-Neu5Ac	Std	614.141	0.89			0.4	
CMP-Neu5Gc	Std	630.131	0.89			0.01	
CMP-KDO	MS/MS, Lit	543.110	0.84				0.4
dTDP-L-Rha	MS/MS, Lit, tent	548.105	1.42				498
dTDP-dhex-2	MS/MS	548.105	1.53				6.2
dTDP-Fuc4NAc	MS/MS, Lit, tent	589.107	1.62				5.5

[1] UDP-GalNAc is presumably present in CHO cells but not separated from UDP-GlcNAc.

Supporting Figures:

SI Figure 1: Selectivity of columns of different age**.** A very new column (**C4**), a column having been used for 3 month with two acid regenaration steps (**C3**) and a rather old PGC column heavily used for a variety of purposes (**C1**) were employed for the separation of a tobacco leaf extract. The upper panel shows the base peak intensity chromatograms of tobacco leaf extracts. Peak labels denote: c, oxidized glutathione; d, UDP-GlcUA; e, UDP-Ara*p*; f, UDP-Rha; g, UDP-Gal; h, UDP-GlcNAc; i, GDP-Man; a, b, and c, unidentified analytes of masses 341, 605 and 630, respectively.

Values derived from duplicate analysis of tobacco leaf extracts - average standard deviation in percent of relative retention time was 0.38 %.

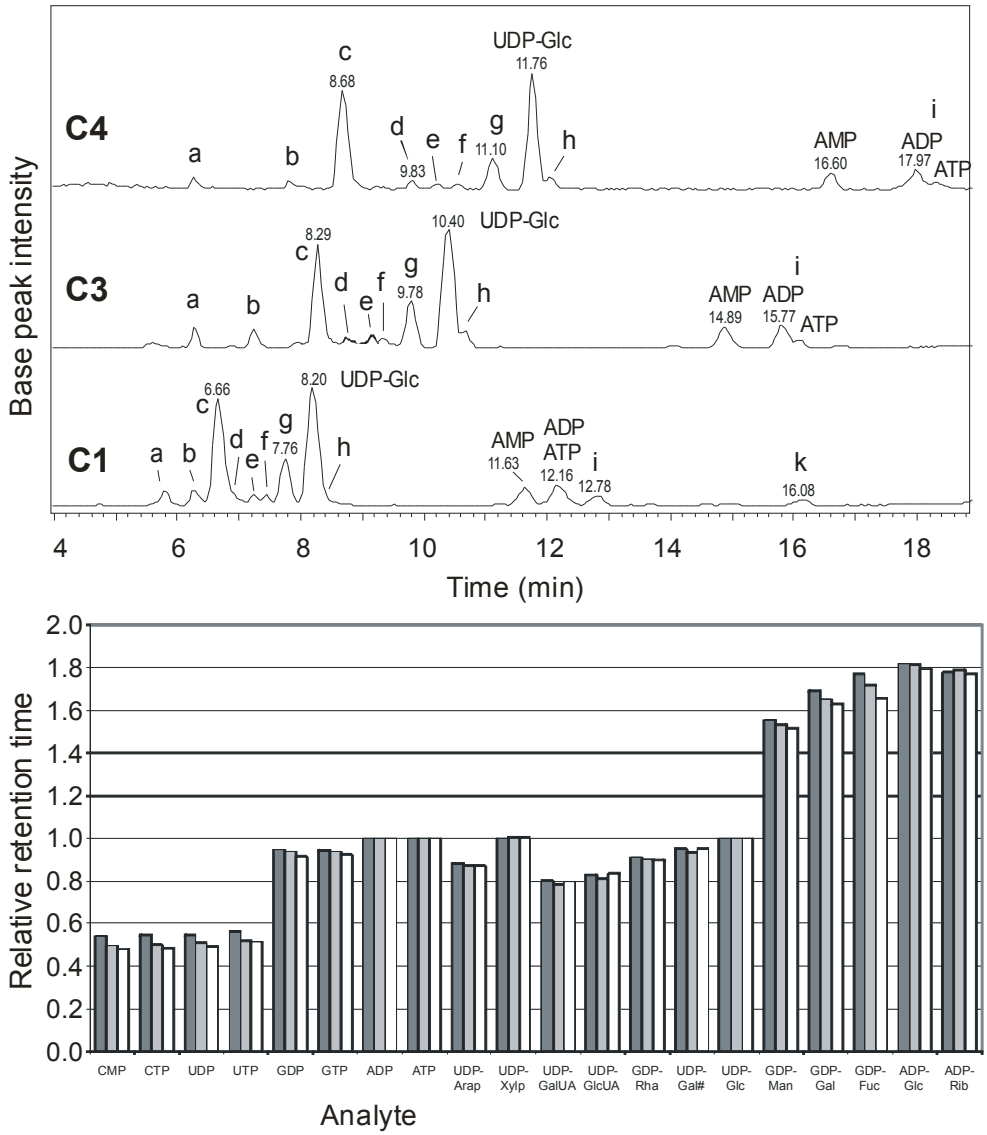

SI Figure 2: CMP-sugars. Panel (**A**) shows the SICs for CMP-Neu5Ac (613.10–613.18 amu) and CMP-Neu5Gc (629.09-629.17) in CHO cells. The insert for Neu5Gc is drawn to scale. Neu5Gc constitutes 1.5 % of activitated sialic acid in CHO cells. Due to its high abundance, oxidized glutathion (GSSG) gives a large signal 2 Da away from its base peak. Panel (**B**) depicts the SIC for CMP-KDO (542.14-542.26) from *E. coli* with the respective MS/MS spectrum showing the CMP fragment.

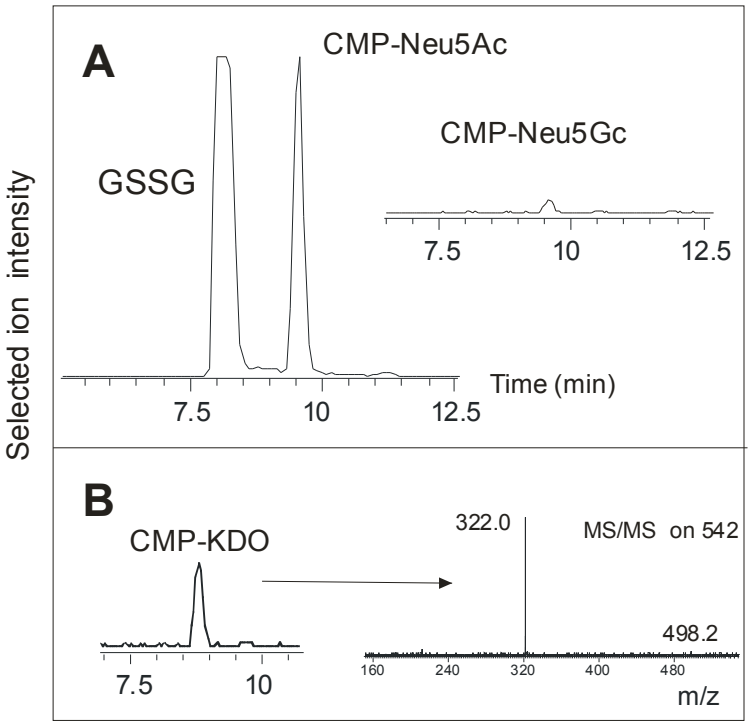

SI Figure 3: GDP-hexoses in *Arabidopsis*. The upper panel (**wt**) depicts the selected ion chromatogram for GDP-hexose with a prominent peak for GDP-Man followed by two smaller peaks representing GDP-L-galactose and, presumably, GDP-L-gulose. The lower panel (**GME**) shows the same SIC for a leave sample from a GME RNAi plant. The insert represents the area ratio of UDP-Gal (white bars), GDP-Man (grey bars) and UDP-Gal+Gul (black bars).

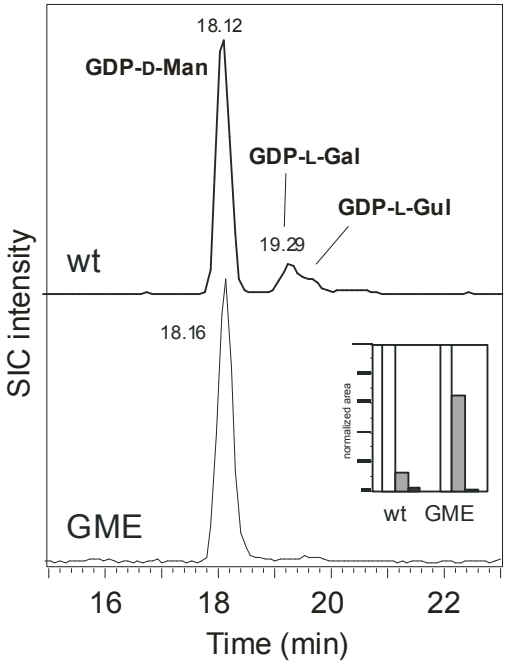

Supporting References

(1) Castilho, A.; Pabst, M.; Leonard, R.; Veit, C.; Altmann, F.; Mach, L.; Glossl, J.; Strasser, R.; Steinkellner, H. *Plant Physiol* **2008**, *147*, 331-339.
(2) Dafny-Yelin, M.; Chung, S. M.; Frankman, E. L.; Tzfira, T. *Plant Physiol* **2007**, *145*, 1272-1281.
(3) Sellick, C. A.; Hansen, R.; Maqsood, A. R.; Dunn, W. B.; Stephens, G. M.; Goodacre, R.; Dickson, A. J. *Anal Chem* **2009**, *81*, 174-183.
(4) Kochanowski, N.; Blanchard, F.; Cacan, R.; Chirat, F.; Guedon, E.; Marc, A.; Goergen, J. L. *Anal Biochem* **2006**, *348*, 243-251.
(5) Fry, S. C.; Northcote, D. H. *Plant Physiol* **1983**, *73*, 1055-1061.
(6) Pabst, M.; Altmann, F. *Anal Chem* **2008**, *80*, 7534-7542.
(7) Konishi, T.; Takeda, T.; Miyazaki, Y.; Ohnishi-Kameyama, M.; Hayashi, T.; O'Neill, M. A.; Ishii, T. *Glycobiology* **2007**, *17*, 345-354.
(8) Anumula, K. R. *Anal Biochem* **1994**, *220*, 275-283.
(9) Leiter, H.; Mucha, J.; Staudacher, E.; Grimm, R.; Glossl, J.; Altmann, F. *J Biol Chem* **1999**, *274*, 21830-21839.
(10) Reiter, W. D. *Curr Opin Plant Biol* **2008**, *11*, 236-243.
(11) Konishi, T.; Ono, H.; Ohnishi-Kameyama, M.; Kaneko, S.; Ishii, T. *Plant Physiol* **2006**, *141*, 1098-1105.
(12) O'Neill, M. A.; Warrenfeltz, D.; Kates, K.; Pellerin, P.; Doco, T.; Darvill, A. G.; Albersheim, P. *J Biol Chem* **1996**, *271*, 22923-22930.
(13) Wolucka, B. A.; Van Montagu, M. *J Biol Chem* **2003**, *278*, 47483-47490.
(14) Major, L. L.; Wolucka, B. A.; Naismith, J. H. *J Am Chem Soc* **2005**, *127*, 18309-18320.
(15) Burkle, A. *Febs J* **2005**, *272*, 4576-4589.
(16) Shull, N. P.; Spinelli, S. L.; Phizicky, E. M. *Nucleic Acids Res* **2005**, *33*, 650-660.
(17) Marolda, C. L.; Valvano, M. A. *J Bacteriol* **1995**, *177*, 5539-5546.
(18) Breazeale, S. D.; Ribeiro, A. A.; McClerren, A. L.; Raetz, C. R. *J Biol Chem* **2005**, *280*, 14154-14167.